FP7-PEOPLE-2013-ITN 607774

ADVanced communicAtions and iNformaTion processing in smArt Grid systems

WP2 D2.2
Initial Findings on Neighbourhood/industry Area Network Research

Status-Version:	Final-1.0
Date:	29/6/2016
EC Distribution:	Public
Project Number:	607774
Project Title:	ADVanced communicAtions and iNformaTion processing in smArt Grid systems

Title of Deliverable:	Initial Findings on Neighbourhood/industry Area Network Research
Date of delivery to the EC:	30/6/2016

Workpackage responsible for the Deliverable	WP2
Lead Editor:	Deep Shrestha
Contributor(s):	Charalampos Kalalas, Deep Shrestha, Mehdi Zeinali
Affiliations	CTTC, UEDIN
Reviewer(s):	Aleksandar Mastilovic, Jesus Alonso-Zarate, John Thompson
Approved by:	All Partners

Abstract	This deliverable provides an overview of the initial findings of the research in NAN and IAN. The results from all three research domains of work package 2 are reported. Specifically, the preliminary results from device-to-device communication, power line communication and smart meter data processing are shown. Furthermore the results are discussed analytically and future research directions are identified.
Keyword List:	Data compression/aggregation, device-to-device communication, power line communication, impulsive noise mitigation, radio resource management, scheduler design

The ADVANTAGE project has received funding from the European Union's Seventh Framework Programme for Research, Technological Development and Demonstration under Grant Agreement 607774.

Document Revision History

Version	Date	Description	Authors
Version 1.0	23 June 2016	Deliverable D2.2	Led by: Jesus Alonso-Zarate Charalampos Kalalas (ESR) Deep Shrestha (ESR) Mehdi Zeinali (ESR) John Thompson (Project Co-ordinator)
Final version	29/06/2016	Final Edits	John S Thompson

Table of Contents

1 Introduction

This work package (WP) focuses on the neighborhood area networks (NANs) and industrial area networks (IANs) of smart grid. Both domains are the key areas where the role of smart grid application becomes prominent and hence real-time, robust and reliable communication solutions are required. To address this challenge, this WP is responsible for exploring the cellular communication and power line communication (PLC) technologies and the requirements in terms of communications and signal processing algorithms to support the smart grid applications in these domains. To elaborate further, cellular technology enables data exchange using the wireless technologies and PLC exploits the existing electrical wires to transmit data where both technologies need to support the communication requirements that are imposed by the smart grid applications.

The initial findings of the research done in the aforementioned directions are reported in three sections of this document. Section 2 provides a brief overview on initial findings of device-to-device communication in terms of radio resource management and scheduler design. Section 3 reports an impulsive noise mitigation scheme that has been proposed in the frame work of power line communication system design for smart grid applications. Finally, section 4 introduces the concept of compression and aggregation of smart meter data that maximizes channel usage efficiency by enabling maximum data transfer using available channel bandwidth.

2 Cellular Communications for Smart Grid NANs

Communication in the power distribution grid already exists at a local level to support basic small-scale automatic operations [1]. However, large-scale operations that involve deployments spanning long distances, e.g., wide-area monitoring, protection and control systems, still rely on extensive human intervention. Moreover, the increasing penetration of distributed energy resources, located in widespread areas, introduces several challenges for achieving efficient and reliable communication [2].

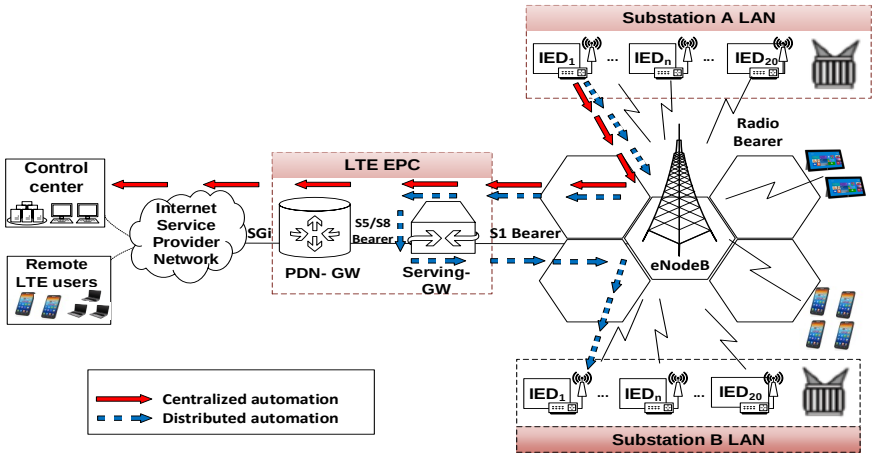

Figure 1: LTE for centralized and distributed substation automation [3].

Among many existing alternatives, cellular technology relying on LTE-based standards (Fig-

ure 1, [3]) has been identified as a promising technology to support advanced and autonomous grid functionalities in NANs/IANs [4]. In this direction, 3GPP standardization efforts, e.g., LTE-M, cat-M1 user category, NB-IoT [5, 6], aim at enabling LTE as a suitable connectivity technology for the machine-type communication and the internet of things (IoT) in the mid-term future. Communication in cellular networks is performed by following two sequential procedures: *i)* the initial network association phase, where devices request transmission resources or re-establish a connection to the eNodeB, i.e., the base station, and *ii)* the actual data transmission phase, where communication may take place either through the eNodeB or via Device-to-Device (D2D), using the resources allocated by the eNodeB in the prior phase. The reliable support of the stringent requirements of distribution grid traffic in shared LTE networks introduces significant challenges in both procedures [4]. Thus, the development of enhanced radio access mechanisms and resource management strategies are the main research goals of our work. In subsections 2.1 and 2.2, we present an overview of the methodologies used until now along with some initial research findings. We also provide an insight on our ongoing work in subsection 2.3.

2.1 Radio Resource Management and Scheduler Design

In the context of ADVANTAGE, we have investigated the reliable support of real-time distribution automation services via public LTE networks. In particular, in our initial work [3], we present the technical and performance requirements introduced by IEC 61850 standard for wide-area substation automation tasks and discuss the ability of LTE to meet these requirements in terms of latency and throughput. As shown in Figure 1, we further focus on the integration of two representative IEC 61850 communication services [7], namely *i*) centralized automation based on Manufacturing Messaging Specification (MMS), where real-time power quality measurements are periodically sent by Intelligent Electronic Devices (IEDs) to a remote controller for system situational awareness and status monitoring, and *ii*) distributed automation based on Generic Object Oriented Substation Event (GOOSE), where time-critical control messages are exchanged between neighboring IEDs that belong to the same or different substation local area networks. As illustrated in our uplink scheduling framework in Figure

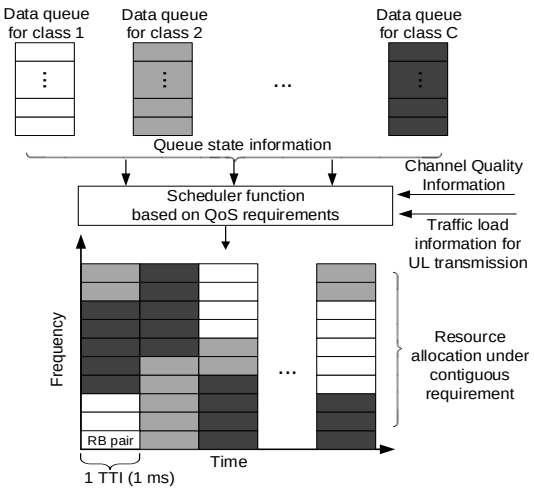

Figure 2: Generic view of the LTE scheduler [3].

2, we address the problem of prioritizing smart grid traffic over conventional human-based services in network overload, by designing an appropriate LTE scheduler that dynamically allocates resources based on an analytical characterization of the performance constraints, while keeping the degradation of LTE subscribers at a minimum level. For the performance evaluation, realistic overload scenarios were considered, where numerous LTE subscribers generate background traffic within the eNodeB coverage area and compete for the available resources with the IEDs.

2.2 Example Results

Our proposed scheduler is compared with the proportional-fair scheduling algorithm for resource allocation, where there is no special handling of smart grid control flow with respect to the other LTE traffic types [3]. Figures 3 and 4 illustrate the superiority of our proposed scheduler for the centralized automation scenario (MMS over LTE). Naturally, this improvement causes some degradation to other types of background traffic, as shown in Figure 5, however performance can still be considered acceptable. In the case of the more demanding distributed automation scenario (GOOSE over LTE), the performance for the control traffic improves, as depicted in Figures 6 and 7. Compared to the first scenario, the impact of prioritized data handling is more visible on background traffic. In particular, while voice delay levels remain low and do not lead to dropped calls, the performance deterioration for video traffic may lead to some unsatisfied video users. However, the overall performance is considered acceptable, since 77% of video frames are now transmitted with less than 0.6 seconds delay, as shown in Figure 8. Network capacity results for both scenarios are illustrated in Tables 1 and 2 respectively.

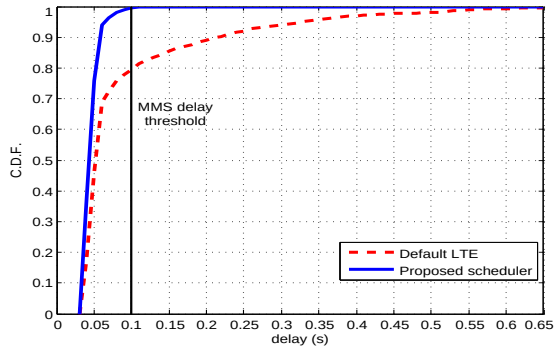

Figure 3: CDF of delay for MMS traffic.

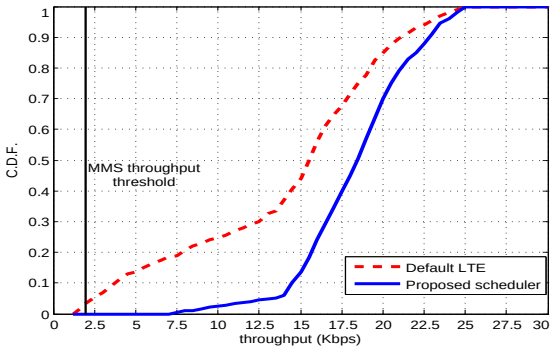

Figure 4: CDF of throughput for MMS traffic.

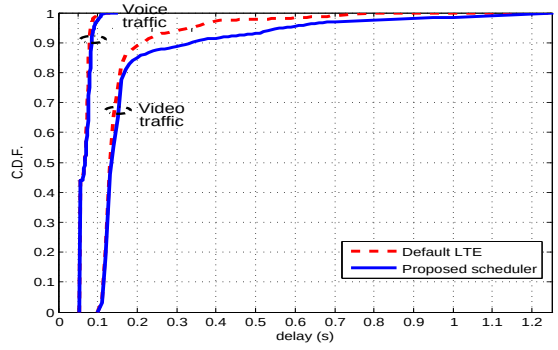

Figure 5: CDF of background voice and video delay in presence of MMS traffic.

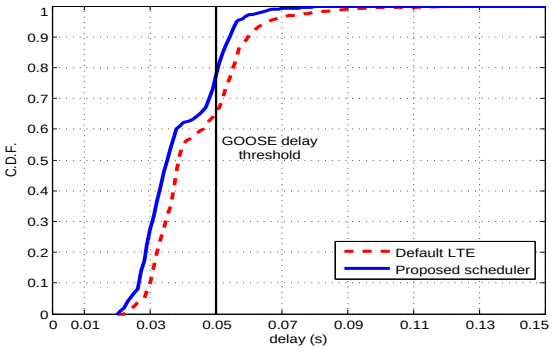

Figure 6: CDF of delay for GOOSE traffic.

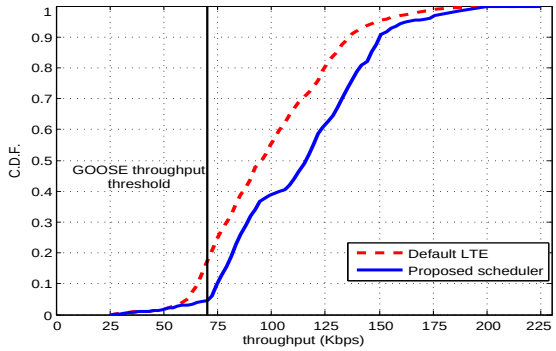

Figure 7: CDF of throughput for GOOSE traffic.

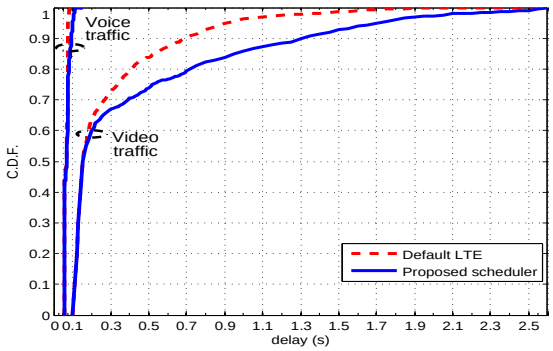

Figure 8: CDF of background voice and video delay in presence of GOOSE traffic.

	Traffic Type				
	Web	VoIP	Video	FTP	MMS
Initial number of active users/IEDs	3	3	1	2	2
Arrival intensity	2.0	3.0	0.75	4.0	1.0
Number of active devices in overload	27	34	15	25	20

Table 1: Network capacity for centralized scenario (MMS over LTE)

	Traffic Type				
	Web	VoIP	Video	FTP	GOOSE
Initial number of active users/IEDs	3	3	1	2	2
Arrival intensity	0.75	1.0	0.75	2.0	0.8
Number of active devices in overload	25	18	29	10	40

Table 2: Network capacity for distributed scenario (GOOSE over LTE)

2.3 Conclusions and Future Work

In our initial work [3], we demonstrate how IEC 61850 standard can be implemented over LTE to extend energy automation services beyond the substation boundaries. Since such time-critical applications are not adequately supported by current LTE implementations, we devised a novel LTE scheduler that prioritizes automation traffic. Our extensive simulations in a system-level simulator indicate that the proposed scheduler enables public LTE infrastructure to efficiently support automation services with minimum impact on background LTE traffic.

Although the 3GPP is incrementally including some support for massive machine-type communication [8, 9], i.e., LTE-M and NB-IoT, the modern cellular system has been basically designed, engineered and managed to afford access only to a reasonable number of conventional LTE subscribers with high downlink data rate. Our future work resides in the investigation of the performance of the LTE Random Access Channel (RACH) for the support of real-time automation services in large-scale distribution grid deployments. The objective is to design an efficient RACH mechanism in order to *i*) handle the traffic surge of simultaneous channel access requests and *ii*) meet the strict latency requirements of mission-critical messages, e.g., the case of cascading power faults where notification alarm messages are triggered. In addition, the performance benefits that direct D2D transmission mode brings to neighboring IEDs will be investigated, along with reliability enhancements for opportunistic channel access.

3 Impulsive Noise Mitigation for PLC Systems

The power lines behave as a frequency selective channel and are severely affected by different types of noise [10, 11]. The noise in power lines is typically classified into background noise, impulsive noise (IN) and narrow band interference (NBI) [11–14]. Among them, the IN is random in occurrence and has a higher power spectral density (PSD) than the background noise and is considered as a major source of error in power line communication (PLC). To mitigate such noise, following information about it needs to be estimated:

- **Order:** The *order* defines the number of IN samples occurring during the transmission.
- **Support:** The *support* defines the time instant of IN sample occurrence.
- **Amplitude:** The *amplitude* of each IN sample occurring during the transmission.

Hence an algorithm that provides precise estimation of above parameters is reported in this section, based on the research published in [15]. To elaborate the scheme, first the system model is defined followed by the order, support and amplitude estimations of IN. Some example results generated by numerical simulations along with the conclusion and future research direction are also provided.

3.1 Asynchronous Impulsive Noise Mitigation Based on Subspace Support Estimation

The complex baseband equivalent discrete-time model for the OFDM based PLC system is written as

$$y = Hx + i + w, \tag{1}$$

where $y \in \mathbb{C}^n$ and $x \in \mathbb{C}^n$ are column vectors that contain the time domain OFDM received and transmitted signals respectively, after cyclic prefix removal. Besides the length of the time domain vectors, n also represents the total number of sub-carriers in the system. Let F denote the $n \times n$ unitary DFT-matrix where $[F]_{a,b} = \frac{1}{\sqrt{n}} \exp^{-j2\pi ab/n}$ with $a, b \in \{0, 1, 2, \ldots, n-1\}$. The notation $[\cdot]$ is used to refer the elements of the matrix or vector inside the bracket. The time domain signal x is transmitted only in k used sub-carriers. Accordingly, the remaining $m = n - k$ are nulled/unused. The transmitted signal vector x is given by $x = F^H S_x X$, where X is a vector of length k containing the frequency domain data symbols. S_x is an $n \times k$ selection matrix having only one element equal to 1 per column indicating used sub-carrier index and m zero rows corresponding to the unused sub carrier. The channel is represented by H, which is an $n \times n$ circulant matrix. w is the background noise of length n, which is defined as a sequence of independent and identically distributed (i.i.d) complex Gaussian random variables with zero mean and variance σ_w^2. The vector i represents IN of length n and its entries $[i]_j$ can be in two states: a state when the IN is active and another state when there is no occurrence of IN. The probability of being at each state is generated as a Bernoulli random variable, whereas the amplitude of the IN itself is assumed Gaussian distributed. Thus, the IN becomes a mixture of Bernoulli and Gaussian random processes. The j^{th} entry of i is modeled as $[i]_j = [b]_j.[g]_j$, where $[b]_j$ is an i.i.d. Bernoulli random variable with probability of success P, and where $[g]_j$ is an i.i.d. complex Gaussian random variable with zero mean and variance I_o. The channel SNR is defined as σ_s^2/σ_w^2, where σ_s^2 is transmitted signal power, whereas the INR is defined as I_o/σ_w^2, where I_o is the IN power.

After receiving the samples as in (1), a Fast Fourier Transform (FFT) is applied. The FFT of vector y is performed by multiplying y by the DFT-matrix F as

$$Y = Fy = DS_x X + Fi + W, \tag{2}$$

where Y is a column vector of length n containing the frequency domain received symbols, $D = diag(\sqrt{n}Fh)$, h being the channel impulse response, and W denoting a vector of length n having the frequency domain transformed samples of the background noise. The contribution from unused sub-carriers is extracted from (2) as

$$Y' = S_x^T Y, \tag{3}$$

where Y' is the column vector of length m corresponding to unused sub-carriers (containing samples from the IN and the background noise only). The vector Y' in (3) is the observation vector for order and support estimation of IN, by employing MDL criterion and MUSIC estimator respectively. After estimating the order and support of IN samples, MMSE estimation of amplitudes at identified supports is performed. The estimated IN samples are then subtracted from the received signal, in (1) before performing the FFT. A block diagram of the proposed scheme is shown in Figure 9.

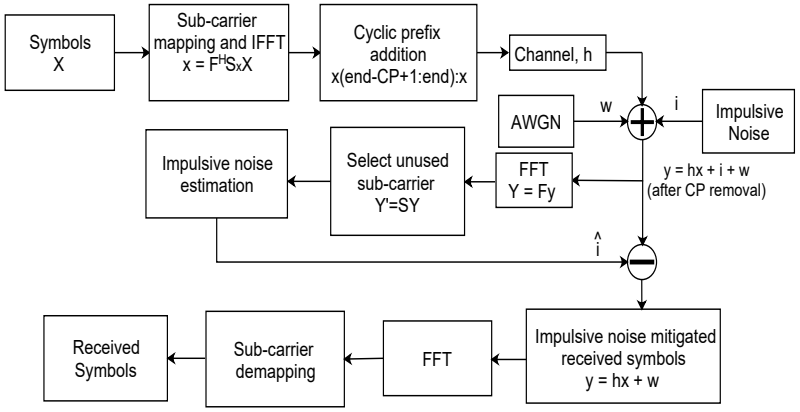

Figure 9: Block diagram of the proposed IN mitigation algorithm.

Order Estimation: Using the samples in Y', a total of $L = m - M + 1$ sample vectors denoted by $\tilde{Y}_l$, where $l \in \{1, 2, 3, \ldots, L\}$, are generated, each having length M. M represents the sample window size that is used to generate the sample covariance matrix, which is chosen such that the condition $M - N > N$ is satisfied, where N is the number of impulses that occur within a multi carrier symbol period. The sample vector $\tilde{Y}_l$ is constructed as

$$\tilde{Y}_l = \left[[Y']_{(l+M-1)}, [Y']_{(l+M-2)}, \ldots, [Y']_l\right]^T \tag{4}$$

The sample covariance matrix $\hat{R}$ of size $M \times M$ is now formed using $\tilde{Y}_l$ as

$$\hat{R} = \frac{1}{L}\sum_{l=1}^{L} \tilde{Y}_l \tilde{Y}_l^H. \tag{5}$$

The eigenvalue decomposition of $\hat{R}$ is performed, resulting into M eigenvectors and M eigenvalues. Out of M eigenvalues arranged in decreasing order $\lambda_1 \geq \lambda_2 \geq \lambda_3 \geq \ldots, \lambda_M$, the N largest are associated with the IN samples whereas the $M - N$ smallest correspond to the background noise samples [16]. By employing the eigenvalues of the sample covariance matrix, we estimate the number of IN impulses by the MDL criterion, according to [17] by

$$MDL(\hat{k}) = -\log\left(\frac{\prod_{r=\hat{k}+1}^{M}\lambda_r^{1/(M-\hat{k})}}{\frac{1}{M-\hat{k}}\sum_{r=\hat{k}+1}^{M}\lambda_r}\right)^{(M-\hat{k})m} + \frac{3\hat{k}}{2}\log\frac{L}{M}. \tag{6}$$

The order N of IN is estimated as the value of $\hat{k} \in \{0, 1, 2, \ldots, M-1\}$ for which (6) bears the minimum value.

Support Estimation: After estimating the IN order, the eigenvector set of $\hat{R}$ is split into two subsets. The first subset contains N eigenvectors that belong to the signal subspace, corresponding to IN. The second subset, defined as the noise subspace $-\{\hat{g}_1, \hat{g}_2, \ldots, \hat{g}_{M-N}\}$, contains $M - N$ eigenvectors corresponding to background noise. The matrix $\hat{G}$ as the column-wise juxtaposition of the eigenvectors in the second subset is defined.

Having identified the noise and signal subspaces, the support set of the IN, $I \in \{d_1, d_2, \ldots, d_N\}$, is estimated as the sample indexes in terms of integers in the set $q \in [0, n-1]$, for which the rational q/n is closest to the peaks of the function $f(t)$ defined as [16]

$$f(t) = \frac{1}{a^H(t)\hat{G}\hat{G}^H a(t)}, t = \frac{q}{n} \in [0, 1), \tag{7}$$

where $q \in \{0, 1, 2, \ldots, n-1\}$ and $a(t)$ is the vector of length M defined as

$$a(t) = [1 \quad e^{it} \ldots e^{i(M-1)t}]^T. \tag{8}$$

Thus identified sample indexes are then arranged in increasing order to appear as entries of I.

Amplitude Estimation: The amplitudes of the IN samples at locations identified by I are estimated using the MMSE criterion. The estimated amplitude of j^{th} IN sample is given by

$$\hat{A}_j = \mathbb{E}([\hat{i}]_j | y, I) = \frac{I_o}{I_o + \sigma_s^2 + \sigma_w^2} y(I), \tag{9}$$

where $j = 1, \ldots, N$, I_o is the IN power, σ_s^2 is the transmitted signal power and σ_w^2 is the background noise power.

Finally, the estimated IN $\hat{i}$ of length n having only N non-zero entries at the supports of IN samples is generated. Upon subtracting this estimate from the time domain received signal vector y in (1) provides an IN-mitigated signal for demodulation as shown in Figure 9.

3.2 Simulation Results

The bit error rate (BER) performance of the proposed IN mitigation scheme and other algorithms (nulling, clipping and time domain periodogram) are evaluated in different scenarios that are defined by the occurrences of impulsive noise with distinct power levels. As shown in Figure 10 and Figure 11 the proposed scheme outperforms the conventional algorithms where the BER of the PLC receiver is improved significantly.

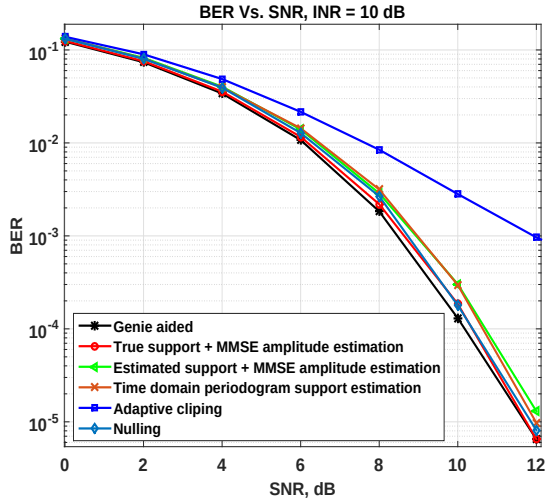

Figure 10: BER performance, INR = 10 dB.

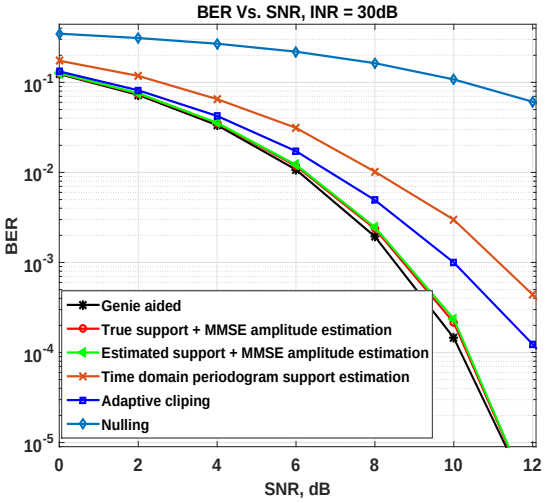

Figure 11: BER performance, INR = 30 dB.

3.3 Conclusion and Future Work

The precise mitigation of impulsive noise in power lines can enhance the performance of PLC systems. This enables the applicability of PLC for smart grid applications by exploiting the electrical grids. Furthermore, the power lines that are often polluted by impulsive noise represent a challenging environment for precise channel estimation. Therefore as the future direction of research, efforts will be made towards designing a robust channel estimator that exploits the knowledge of estimated impulsive noise.

4 Introduction to Impact of Compression and Aggregation in Wireless Networks on Smart Meter Data

Smart meters record and transmit information regarding the consumed electricity at rates of seconds to hours.There are two methods for smart meter communication suggested in the literature. The first scenario is to use the wireless cellular network for smart meter communication by adding communication modules to the smart meters. The second scenario is to implement a wireless sensor network technology which builds a communication link through a mesh network of smart meters [18]. In this section, the study done considering the first scenario where smart meters are directly connected to the wireless cellular network is presented. Reducing the network load decreases operational costs and due to the very large data volumes of energy data, compression will be a necessary technique. The most important reasons for compression are [19]:
i) Reducing data volume
ii) Communication bandwidth efficiency
iii) Improving energy efficiency by reduction in data volume for wireless transmission
The findings illustrated here are a summary of the research to be presented at the IEEE SPAWC 2016 conference [20]. We evaluate two different lossless compression techniques at the smart meter side. The basic concept of data compression and different communication

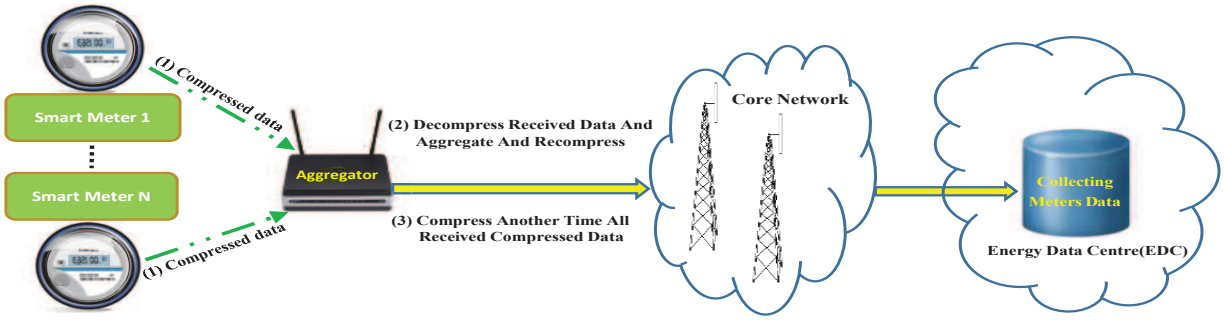

Figure 12: Metering infrastructure and network topology showing the aggregation scenarios 1,2 and 3.

and aggregation scenarios for our work are presented in the upcoming subsection and the last two subsections respectively define the results for data compression using real world datasets and conclusions with future research directions.

4.1 Data Compression and Simulation Scenarios

The basic idea behind data compression technique is to remove data redundancy by encoding it more efficiently. By doing so, less disk memory will be used for data storage and less bandwidth of the channel will be used to transmit the same amount of data [19]. The concept of data compression is categorized in two main groups, namely: lossy and lossless compression. In lossy compression the fidelity of the data is reduced when it is decompressed, whereas lossless compression algorithms reduces the data volume without any loss of data and the result after decompression is a bit-for-bit match with the original information. The evaluation of different techniques is done in terms of compression ratio and compression time. The compression ratio that determines the compression efficiency of a technique is defined as the ratio of data size before and after compression and is expressed as:

$$\mathrm{CompressionRatio} = \frac{(\mathrm{UncompressedSize})}{(\mathrm{CompressedSize})} \tag{10}$$

In this work, two data compression techniques Lempel-Ziv-Welch (LZW) [21,22] and Adaptive Huffman (AH) [23, 24] are studied. To perform the evaluation three scenarios that use different compression strategies are assumed and are shown in Figure. 12. In the first scenario, compressed smart meter data are sent to aggregator, which are simply forwarded directly to energy data center (EDC) through internet without further processing. In the second scenario, the aggregator receives the compressed data from each smart meter and decompresses it, such that it can be aggregated with a group of other data packets to form a large data packet which is later compressed again. In the third scenario, the received compressed smart meter data are aggregated and further compression is done without decompressing them.

In order to evaluate smart meter data compression, we analyzed different data sets obtained from low frequency Massachusetts Institute of Technology (MIT) Reference Energy Disaggregation Data Set (REDD) [25]. This data set contains a total of 116 readings taken at

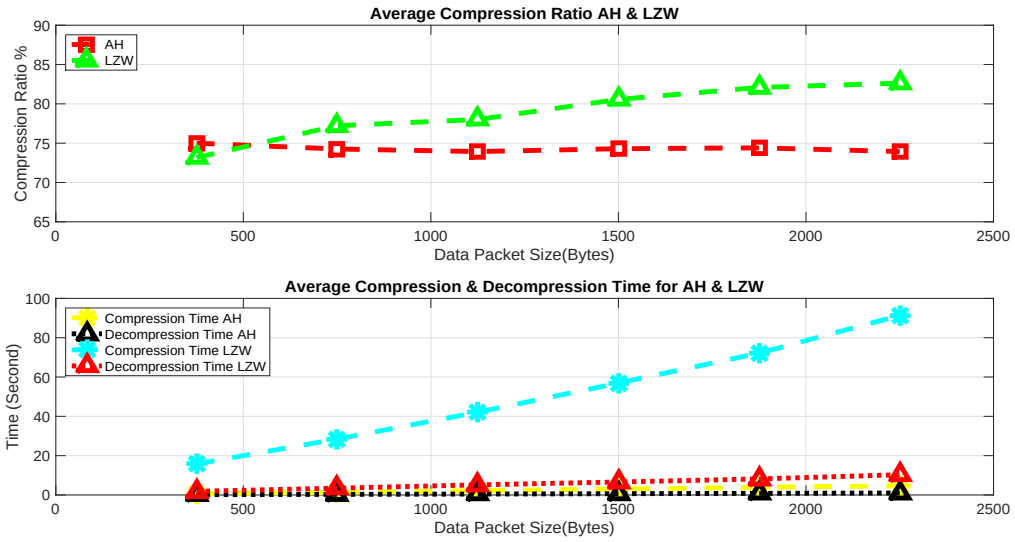

Figure 13: Average compression ratio (top figure) and average compression time (bottom figure) for LZW and AH algorithm applied to meter data in 10 mins intervals (scenario 1).

household and circuit level from six different houses. The data sampling interval is 1 second with a resolution of 0.01 watts.

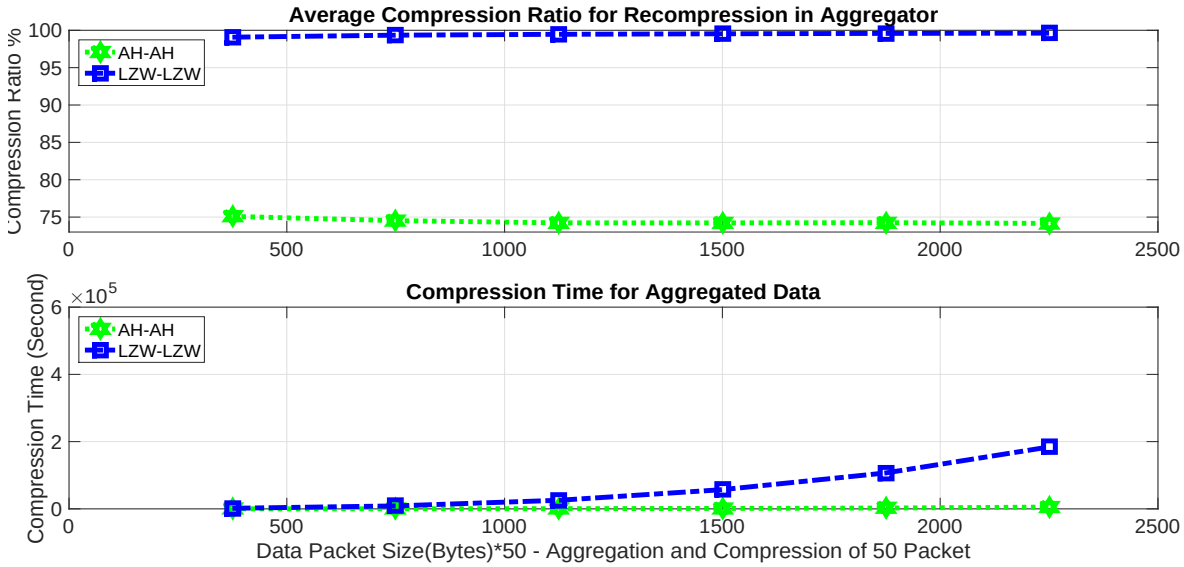

Figure 14: Results for compression ratio (top figure) and compression time (bottom figure) vs packet size for decompression in the aggregator followed by compression of aggregated data (scenario 2).

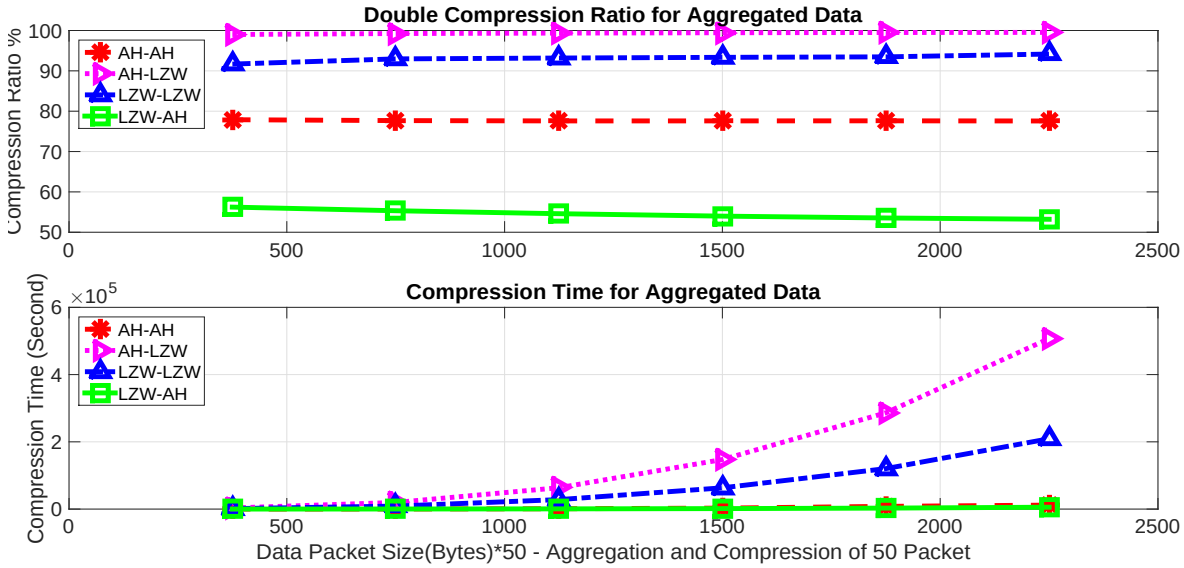

Figure 15: Results for compression ratio (top figure) and compression time (bottom figure) vs packet size for double compression without decompression in aggregator (scenario 3).

4.2 Results and Discussion

The LZW and AH compression techniques have been applied to smart meter data and two important parameters, compression gains and processing time have been evaluated for those algorithms. Our investigation on smart meter data shows that smart meter data can be significantly compressed in size by these compression algorithms. The effect of compressing is investigated by considering different reading types and dataset sizes. Figure. 13 shows the compression rates, compression and decompression times for the first simulation scenario where only the smart meters compress data. The applied techniques achieve average compression rates of 74-88 while using LZW method. If low execution time is mandatory, the AH algorithm is the best choice and it can achieve an average 74% compression rate for all packet sizes. If the compressed data from the smart meters is decompressed in the aggregator and aggregated into a single data packet, we can then recompress this larger data packet (comprising 50 packets from 50 smart meters) to achieve a higher overall compression ratio. This is the second scenario for simulation and results are shown for both meters and aggregators using AH (AH-AH) or LZW (LZW-LZW) in Figure. 14. Figure. 15 depicts the third communication scenario that shows combination of both compression techniques at different points in the communication topology. The results show that the best compression ratio is obtained when LZW technique is applied in the aggregator after AH compression on smart meter.

4.3 Conclusion and Future Work

This work has investigated the performance of compression and aggregation techniques for smart meter data. For large dataset sizes, the LZW algorithm achieved higher compression rate and consequently bandwidth of channel can be efficiently utilized, at the cost of com-

plexity. The AH algorithm with a lower processing time could save more energy consumption, processing time and hardware requirements when implemented in smart meters. Selecting the desired trade-off between compression rate, processing time and hardware requirements will determine the best compression algorithm for each part of our communication scenario. As a future work, alternative compression algorithms to the LZW and AH methods will be investigated while the effect of errors and packet losses on the communication channels will also be considered.

5 WP2 - Overall Conclusions

The initial findings on NAN and IAN research have been reported. The results presented in this document provide an overview of the solutions for both D2D communication and PLC in the context of smart grid. In addition, brief insights on data compression techniques to efficiently minimize smart meter data packet sizes have also been reported. After the analytical overview of the initial results, future research directions for all three domains of WP2 have been determined.

References

[1] P. Parikh, T. Sidhu, and A. Shami, "A Comprehensive Investigation of Wireless LAN for IEC 61850-Based Smart Distribution Substation Applications," *Industrial Informatics, IEEE Transactions on*, vol. 9, no. 3, pp. 1466–1476, Aug. 2013.

[2] A. Timbus, M. Larsson, and C. Yuen, "Active management of distributed energy resources using standardized communications and modern information technologies," *Industrial Electronics, IEEE Transactions on*, vol. 56, no. 10, pp. 4029–4037, Oct. 2009.

[3] C. Kalalas, L. Gkatzikis, C. Fischione, P. Ljungberg, and J. Alonso-Zarate, "Enabling IEC 61850 Communication Services over Public LTE Infrastructure," in *Proc. IEEE Int. Conf. Commun. (ICC)*, May 2016, pp. 1–6.

[4] C. Kalalas, L. Thrybom, and J. Alonso-Zarate, "Cellular Communications for Smart Grid Neighborhood Area Networks: A Survey," *IEEE Access*, vol. 4, pp. 1469–1493, Apr. 2016.

[5] 3GPP TS 22.368 v12.1.0, "Service requirements for Machine-Type Communications (MTC) Stage 1," Dec. 2012, Release 12.

[6] 3GPP TR 45.820 V13.0.0, "Cellular system support for ultra-low complexity and low throughput Internet of Things (CIoT)," Tech. Rep., 2015.

[7] IEC, "IEC 61850 Part 8-1: Specific Communication Service Mapping (SCSM) - Mappings to MMS (ISO 9506-1 and ISO 9506-2) and to ISO/IEC 8802-3," Jun. 2011.

[8] 3GPP TR 37.868 v11.0.0, "Study on RAN improvements for Machine-Type Communications," Sep. 2011.

[9] A. Laya, L. Alonso, and J. Alonso-Zarate, "Is the Random Access Channel of LTE and LTE-A Suitable for M2M Communications? A Survey of Alternatives," *Communications Surveys Tutorials, IEEE*, vol. 16, no. 1, pp. 4–16, Feb. 2014.

[10] M. Zimmermann and K. Dostert, "A multipath model for the powerline channel," *IEEE Transactions on Communications*, vol. 50, no. 4, pp. 553–559, Apr 2002.

[11] ——, "Analysis and modeling of impulsive noise in broad-band powerline communications," *IEEE Transactions on Electromagnetic Compatibility*, vol. 44, no. 1, pp. 249–258, Feb 2002.

[12] N. Andreadou and F. Pavlidou, "PLC channel: Impulsive noise modelling and its performance evaluation under different array coding schemes," *IEEE Transactions on Power Delivery*, vol. 24, no. 2, pp. 585–595, April 2009.

[13] M. Katayama, T. Yamazato, and H. Okada, "A mathematical model of noise in narrowband power line communication systems," *IEEE Journal on Selected Areas in Communications*, vol. 24, no. 7, pp. 1267–1276, July 2006.

[14] M. Gotz, M. Rapp, and K. Dostert, "Power line channel characteristics and their effect on communication system design," *IEEE Communications Magazine*, vol. 42, no. 4, pp. 78–86, Apr 2004.

[15] D. Shrestha, X. Mestre, and M. Payaro, "Asynchronous impulsive noise mitigation based on subspace support estimation for plc systems," in *in proceedings of 2016 International Symposium on Power Line Communications and its Applications (ISPLC)*, March 2016.

[16] P. Stoica and R. Moses, *Introduction to Spectral Analysis*. Upper Saddle River, New Jersey, USA: Prentice Hall, 1997.

[17] M. Wax and T. Kailath, "Detection of signals by information theoretic criteria," *IEEE Transactions on Acoustics Speech and Signal Processing*, vol. 33, no. 2, pp. 387–392, Apr 1985.

[18] A. Unterweger and D. Engel, "Resumable load data compression in smart grids," *IEEE Transactions on Smart Grid*, vol. 6, no. 2, pp. 919–929, March 2015.

[19] M. Ringwelski, C. Renner, A. Reinhardt, A. Weigel, and V. Turau, "The hitchhiker's guide to choosing the compression algorithm for your smart meter data," in *Energy Conference and Exhibition (ENERGYCON), 2012 IEEE International*, Sept 2012, pp. 935–940.

[20] M. Zeinali and J. Thompson, "Impact of compression and aggregation in wireless networks on smart meter data," in *in proceedings of IEEE International workshop on Signal Processing advances in Wireless Communications*, Jul 2016.

[21] J. Ziv and A. Lempel, "A universal algorithm for sequential data compression," *IEEE Transactions on Information Theory*, vol. 23, no. 3, pp. 337–343, May 1977.

[22] T. A. Welch, "A technique for high-performance data compression," *Computer*, vol. 17, no. 6, pp. 8–19, June 1984.

[23] D. A. Huffman, "A method for the construction of minimum-redundancy codes," *Proceedings of the IRE*, vol. 40, no. 9, pp. 1098–1101, Sept 1952.

[24] J. S. Vitter, "Design and analysis of dynamic huffman coding," in *Foundations of Computer Science, 1985., 26th Annual Symposium on*, Oct 1985, pp. 293–302.

[25] J. Z. Kolter and M. J. Johnson, "Design and analysis of dynamic huffmaredd: A public data set for energy disaggregation research," in *in proceedings of the SustKDD workshop on Data Mining Applications in Sustainability*, 2011.